Bayesian Inference Applied to the Electromagnetic Inverse Problem

D. M. Schmidt, J. S. George, and C. C. Wood (P-21)

Introduction

Under suitable conditions of spatial and temporal synchronization, neuronal currents are accompanied by electric potentials and magnetic fields that are sufficiently large to be recorded noninvasively from the surface of the head. Such recordings are known as electroencephalograms (EEGs) and magnetoencephalograms (MEGs), respectively. In contrast to positron emission tomography (PET) and functional magnetic resonance imaging (fMRI), which measure cerebral vascular changes secondary to changes in neuronal activity, EEG and MEG are direct physical measurements of neuronal currents and are capable of resolving temporal patterns of neural activity in the millisecond range.[1,2,3] However, unlike PET and fMRI, the problem of estimating current distribution in the brain from surface EEG and MEG measurements (the so-called electromagnetic inverse problem) is mathematically ill-posed; that is, it has no unique solution in the most general, unconstrained case.[4,5]

To address this difficulty of EEG and MEG, we have developed a new probabilistic approach to the electromagnetic inverse problem[6] based on Bayesian inference (see, *e.g.*, Bernardo and Smith[7] and Gelman, *et al.*[8]). Unlike other approaches to this problem, including other recent applications of Bayesian methods[9,10], our approach does not result in a single "best" solution. Rather, we estimate a probability distribution of solutions upon which all subsequent inferences are based. This distribution provides a means of identifying and estimating the likelihood of current-source features using surface measurements that explicitly emphasize the multiple solutions that can account for any set of surface EEG/MEG measurements.

In addition to emphasizing the inherent probabilistic character of the electromagnetic inverse problem, Bayesian methods provide a formal, quantitative means of incorporating additional relevant information, independent of the EEG/MEG measurements themselves, into the resulting probability distribution of inverse solutions. Such information can include constraints derived from anatomy on the likely location and orientation of current[9,11,12,13], maximum current strength, spatial and temporal smoothness of current, *etc.*

Bayesian Inference

Bayesian inference (BI) is a general procedure for constructing a posterior probability distribution for quantities of interest from the measurements, given prior probability distributions for all of the uncertain parameters—both those that relate the quantities of interest to the measurements and the quantities of interest themselves. The method is conceptually simple, using basic laws of probability. This makes its application even to complicated problems relatively straightforward. The posterior probability distribution is often too complicated to be calculated analytically, but can usually be adequately sampled using modern computer

techniques, even in problems with many parameters. More detailed discussions of Bayesian inference can be found elsewhere (*e.g.*, Gelman, *et al.*[8]).

Activity Model

The methods of BI applied to the EEG/MEG inverse problem are demonstrated within the context of a model for the regions of activation. This model is intended to be applicable in evoked-response experiments. There is both theoretical and experimental evidence that EEG and MEG recorded outside the head arise primarily from neocortex, in particular from apical dendrites of pyramidal cells (see, for example, Hämäläinen, *et al.*[1]; Allison, *et al.*[14]; and Dale and Sereno[15]). We therefore construct a model that assumes a variable number of variable-size cortical regions of stimulus-correlated activity in which current may be present. Specifically, an active region is assumed to consist of those locations which are identified as being part of cortex and are located within a sphere of some radius, r, centered on some location, w, also in cortex. There can be any number, n, of these active regions up to some maximum, n_{max}, and the radius can have any value up to some maximum, r_{max}. The goal is to determine the posterior probability values for the set of activity parameters, $\alpha = \{n,w,r\}$, which govern the number, location, and extent of active regions.

Examples

While the methods described apply to models for both EEG and MEG data, the remainder of this research highlight will use MEG data to illustrate the properties of the approach. Both simulated and empirical MEG data for a Neuromag-122 whole-head system were used.[16] The physical setup of the actual MEG experiment was used to determine the location of the subject's head relative to the sensors in the simulated data examples. In addition, an anatomical MRI data set acquired from the subject in the MEG experiment was used to determine the location of cortex (actually gray matter) using MRIVIEW (see Fig. 1), a software tool developed in our laboratory.[17] About 50,000 voxels were tagged, and the normal directions for each of these voxels was then determined by examining the curvature of the local tagged region.

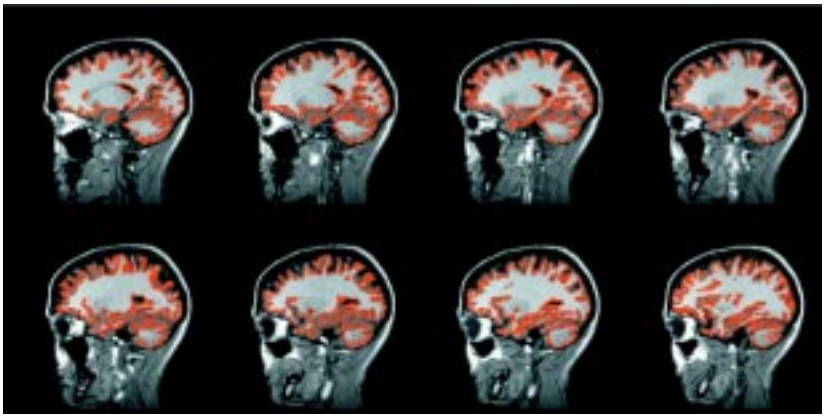

Fig. 1 Gray matter regions are tagged (in red) from anatomical MRI data. These tagged voxels constitute the anatomical model used to implement the cortical location and orientation prior information.

In the first example, a simulated data set was generated using the three active regions of different sizes shown in Fig. 2. Normally distributed noise was added to the simulated data at a level typical of empirical experiments. Our Bayesian inference analysis was applied to this data, and ten thousand samples of the posterior probability were generated. A few of these samples are shown in Fig. 3. All of the samples shown in Fig. 3 are among the 95% most probable and therefore fit both the data and the prior expectations quite well. Any of these could have produced the given simulated MEG data, yet there are clearly vast differences among the samples. The number of active regions ranges from 3 to 6, the sizes of the regions vary greatly, and the locations of the active regions vary across nearly the entire tagged region of the brain (when considering all samples). This variability is a representation of the degree of the ambiguity of the inverse problem for these MEG data, even with the prior information present.

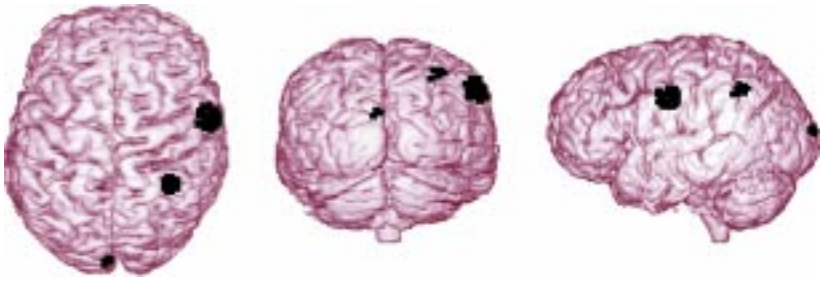

Fig. 2 Maximum intensity projections of the location and extent of the active regions used to generate the simulated MEG data from the first example.

Despite the degree of variability among the samples in Fig. 3, features common to all are apparent; namely active regions within the three general areas used to generate the simulated data (see Fig. 2). Features such as these, common to all or most of the samples, are associated with a high degree of probability. This

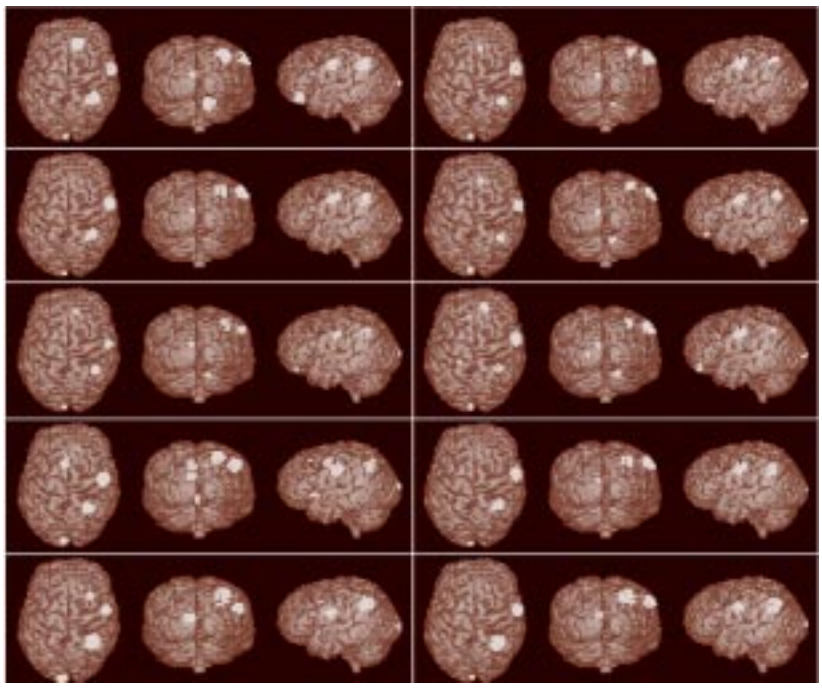

Fig. 3 A few of the samples drawn from the posterior probability distribution for the simulated data in the first example. Each panel shows three views of the maximum intensity projection of all of the active regions from a single sample. Any of these samples could have produced the given MEG data set.

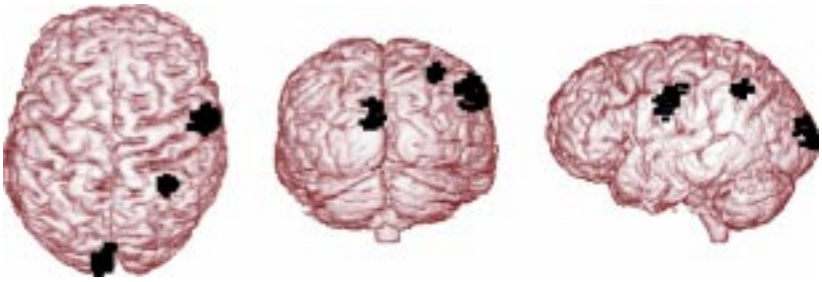

Fig. 4 Three views of the maximum-intensity projections of the location and extent of the three regions found to contain centers of activity at a probability level of at least 95% in the first example.

probability can be quantified because the samples are distributed according to the posterior probability distribution. The smallest sets of voxels that contained the center of the active regions in these three areas across 95% of the samples were identified and are shown in Fig. 4. While these regions are consistent with the locations of the active regions used to generate the simulated data, what is more important is that these regions are consistent with at least 95% of the likely sets of active regions that could also have been generated with this data. This is true even when allowing a variable number of active regions of variable extent. This is a very important feature of BI which is necessarily missing from any other analysis method that only considers one possible result, even if it happens to be the most likely result within a given model.

To learn about the extent and size of each of the active regions localized in Fig. 4, we generated a histogram of the radius of the active regions in each of the areas shown in Fig. 4 across the samples (see Fig. 5). This represents the posterior probability for the size of active regions, assuming there was an active region in each of these areas. The radii of the actual regions used to generate the data were 8, 5, and 3 mm in anterior to posterior order. The agreement between actual radii and posterior probabilities is especially remarkable given the variation in the current strengths of the regions used to generate the data. Such information on extent can be very useful, is not present in most other current methods for analyzing MEG data, and is affirmation of the likely utility of anatomical and physiological prior information.

In our second example, we compared Bayesian analyses of MEG responses to visual stimuli in the left and right visual fields to examine the sensitivity of the Bayesian approach in detecting known features of human visual cortex organization.[18] Based on the crossed anatomical projections of the visual fields to the brain and on previous lesion, MEG, and fMRI studies in humans (see, for example, Horton and Hoyt[19]; Sereno, *et al.*[20]; and Aine, *et al.*[21]), initial cortical activation for stimuli in the left and right visual fields should occur near the calcarine fissure in the occipital region of the contralateral hemispheres.

Fig. 5 The posterior probability distributions for the size of the three active regions whose centers are shown in Fig. 4 in anterior to posterior order. The true sizes of the regions used to generate the simulated data were 8 mm (a), 5 mm (b), and 3 mm (c).

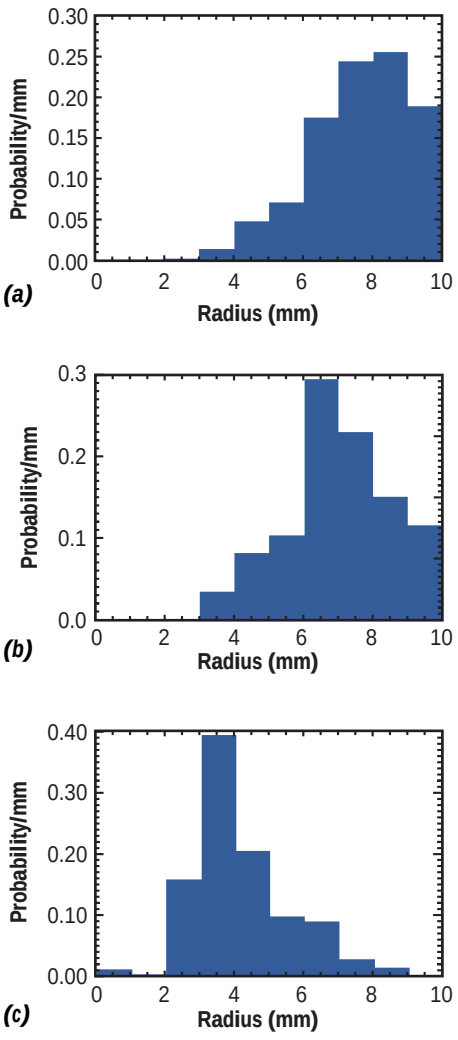

Our Bayesian inference analysis was applied separately to the data for each visual field stimulus at 110-ms post-stimulus latency, a latency that should include robust activation of the calcarine region.[21] Regions that contained activity at a probability of 95% were identified and are shown in Fig. 6. This figure depicts relative probability of activation within these regions on a color scale in three orthogonal slices through the calcarine region and a three-dimensional (3-D) rendering of the occipital region. For the left visual field stimulus, maximal probability of activation at 110 ms was located in the right (contralateral) hemisphere, centered on the calcarine region. This pattern was reversed for the right visual field stimulus at 110 ms, consistent with the predictions from anatomy and from the lesion, fMRI, and previous MEG studies cited above.

Two additional features of the results in this second example should be noted. First, although maximal probability of activation at 110-ms latency was indeed located in the opposite hemisphere, there exists sizable probability for activity in the ipsilateral hemisphere near the mid-line. The extent of the 95% probability regions shown in Fig. 6 is indicative of both the extent of estimated activation and the degree of error or uncertainty in that estimate, even allowing for the possibility of different numbers of active regions of variable extent. Second, although not shown in detail here, analyses at other latencies suggest a progressively increasing number of probable regions of activation in both the ipsilateral and contralateral hemispheres over the latency region from 110 to 160 ms following stimulus onset. It will be of considerable interest to explore the time dependence of the Bayesian inference analyses in relation to evidence for multiple, functionally organized areas of striate and extra-striate visual cortex and to examine the value of temporal prior information (not included in the current activation model) in the form of, for example, temporal covariance constraints.

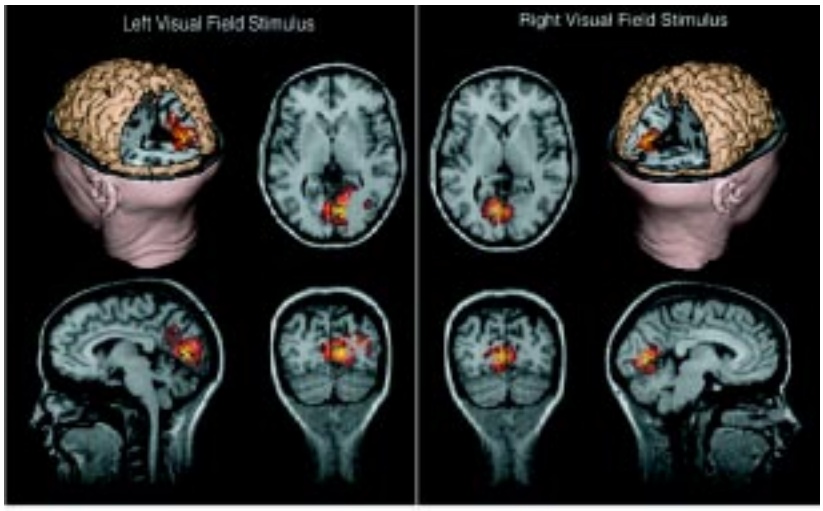

Fig. 6 Four views of a region found to contain activity at a 95% probability level in the second example for both left and right visual field stimuli at 110-ms latency. The two-dimensional views show the regions within the anatomical MRI data using a temperature-like color scale (bright yellow represents the highest probability). The 3-D views show the locations of the regions relative to other brain structures. These results indicate that the highest probability of activity is in the calcarine region of the hemisphere contralateral to the visual field stimulated.

In addition, the Bayesian approach provides a natural means for incorporating information from other functional imaging modalities such as PET or fMRI.[12,13,22] The latter can be readily achieved with the Bayesian framework and with this activity model by assigning prior probabilities to possible locations of active regions based on results from the other modality or modalities. Such a Bayesian formulation of multimodality integration would yield an inherently probabilistic result in which the quantity estimated would be the probability of activation as a function of both space and time.

References

[1] M. Hämäläinen, R. Hari, R. J. Ilmoniemi, J. Knuutila, and O. V. Lounasmaa, "Magnetoencephalography—Theory, Instrumentation, and Applications to Noninvasive Studies of the Working Human Brain," *Review of Modern Physics* **65**, 413 (1993).

[2] C. J. Aine, "A Conceptual Overview and Critique of Functional Neuroimaging Techniques in Humans: MRI/fMRI and PET," *Critical Reviews in Neurobiology* **9**, 229 (1995).

[3] A. W. Toga and J. C. Mazziotta, *Brain Mapping: The Methods* (Academic Press, New York, 1996).

[4] H. von Helmholtz, "Ueber einige gesetze der vertheilung elektrischer strome in korperlichen leitern, mit anwendung auf die thierisch-elektrischen versuche," *Annalen der Physik und Chemie* **89**, 211 and 353 (1853).

[5] P. Nunez, *Electrical Fields of the Brain: Neurophysics of the EEG* (Oxford University Press, Oxford, 1981).

[6] D. M. Schmidt, J. S. George, and C. C. Wood, "Bayesian Inference Applied to the Electromagnetic Inverse Problem," Los Alamos National Laboratory report LA-UR-97-4813 (1997). To be published in *Human Brain Mapping*.

[7] J. M. Bernardo and A. F. M. Smith, *Bayesian Theory* (Wiley, New York, 1994).

[8] A. Gelman, J. B. Carlin, H. S. Stern, and D. B. Rubin, *Bayesian Data Analysis* (Chapman & Hall, London, 1995).

[9] S. Baillet and L. Garnero, "A Bayesian Approach to Introducing Anatomo-Functional Priors in the EEG/MEG Inverse Problem," *IEEE Transactions on Biomedical Engineering* **44**, 374 (1997).

[10] J. W. Phillips, R. M. Leahy, and J. C. Mosher, "MEG-Based Imaging of Focal Neuronal Current Sources," *IEEE Transactions on Medical Imaging* **16**, 338 (1997).

[11] J. Z. Wang, S. J. Williamson, and L. Kaufman, "Magnetic Source Images Determined by a Lead-Field Analysis: the Unique Minimum-Norm," *IEEE Transactions on Biomedical Engineering* **39**, 665 (1992).

[12] J. S. George, C. J. Aine, J. C. Mosher, D. M. Schmidt, D. M. Ranken, H. A. Schlitt, C. C. Wood, J. D. Lewine, J. A. Sanders, and J. W. Belliveau, "Mapping Function in the Human Brain with MEG, Anatomical MRI, and Functional MRI," *Journal of Clinical Neurophysics* **12**, 406 (1995).

[13] A. M. Dale, "Strategies and Limitations in Integrating Brain Imaging and Electromagnetic Recording" *Society for Neuroscience Abstracts* **23**, 1 (1997).

[14] T. Allison, C. C. Wood, and G. McCarthy, "The Central Nervous System," in *Psychophysiology: Systems, Processes and Applications: A Handbook*, E. Donchin, S. Porges, and M. Coles, Eds. (Guilford Press, New York, 1986), pp. 5–25.

[15] A. M. Dale and M. I. Sereno, "Improved Localization of Cortical Activity by Combining EEG and MEG with MRI Cortical Surface Reconstruction: a Linear Approach," *Journal of Cognitive Neuroscience* **5**, 162 (1993).

[16] A. I. Ahonen, M. S. Hämäläinen, M. J. Kajola, J. E. T. Knuutila, P. P. Laine, O. V. Lounasmaa, L. T. Parkkonen, J. T. Simola, and C. D. Tesche, "122-Channel SQUID Instrument for Investigating the Magnetic Signals from the Human Brain," *Physica Scripta* **T49A**, 198 (1993).

[17] D. M. Ranken and J. S. George, "MRIVIEW: An Interactive Computational Tool for Investigation of Brain Structure and Function," in *Visualization '93* (IEEE Computer Society, 1993), pp. 324–331.

[18] C. Aine, H. W. Chen, D. Ranken, J. Mosher, E. Best, J. George, J. Lewine, and K. Paulson, "An Examination of Chromatic/ Achromatic Stimuli Presented to Central/Peripheral Visual Fields: An MEG Study," *Neuroimage* **5**, 153 (1997).

[19] J. C. Horton and W. F. Hoyt, "The Representation of the Visual Field in Human Striate Cortex," *Proceedings of the Royal Society of London* 132, 348 (1991).

[20] M. I. Sereno, A. M. Dale, J. B. Reppas, K. K. Kwong, J. W. Belliveau, T. J. Brady, B. R. Rosen, and R. B. H. Tootell, "Borders of Multiple Visual Areas in Human Revealed by Functional Magnetic Resonance Imaging," *Science* 268, 889 (1995).

[21] C. Aine, S. Supek, J. George, D. Ranken, J. Lewine, J. Sanders, E. Best, W. Tiee, E. Flynn, and C. C. Wood, "Retinotopic Organization of Human Visual Cortex: Departures from the Classical Model," *Cerebral Cortex* 6, 354 (1996).

[22] J. Belliveau, "Dynamic Human Brain Mapping using Combined fMRI, EEG and MEG," Symposium on Approaches to Cognitive Neuroscience by Means of Functional Brain Imaging (Caen, France, 1997).